

Investigation of Surfactant Conformation and Order at the Liquid–Liquid Interface by Total Internal Reflection Sum-Frequency Vibrational Spectroscopy

John C. Conboy, Marie C. Messmer,[†] and Geraldine L. Richmond*

Department of Chemistry, University of Oregon, Eugene, Oregon 97403

Received: December 4, 1995[⊗]

The conformational order of sodium dodecyl sulfate (SDS) adsorbed at the D₂O–CCl₄ interface has been examined by total internal reflection sum-frequency vibrational spectroscopy. A change in conformation of the alkyl chain with increased surface coverage at the liquid–liquid interface is observed. A series of aqueous surfactant concentrations have been examined in order to determine the effect of surface coverage on the conformation of the alkyl chains at the interface. Polarization studies indicate that, for the concentration range examined, the symmetry axis of the terminal methyl group on the alkyl chain is oriented primarily along the surface normal. Identification of spectral features in the C–H region of the infrared region is facilitated by examination of the sum-frequency spectrum from an analogous deuterated compound.

Introduction

Intermolecular forces play a large role in reactivity, orientation, and structural conformation in molecular systems. At surfaces and interfaces, molecules possess unique properties, undergoing reactions and ordering caused by the asymmetric nature of the interfacial region.^{1,2} In recent years there has been increased interest in the adsorption, molecular structure, and electrochemical properties of molecules at liquid interfaces. The interface between two immiscible liquids has proven to be a particularly difficult surface to characterize due to the inability to access this interface with conventional techniques which provide molecular level information. What is known has primarily come from techniques that probe only macroscopic properties of the interface such as interfacial tension and electrochemical and transport properties. Much more remains to be learned about this interface concerning molecular conformation and adsorption in the interfacial region.

Molecular adsorption at liquid–liquid interfaces plays an important role in many biological and chemical systems such as biological membranes, extraction processes, and electron transfer.^{1,2} While studies have been done to investigate the orientation and adsorption of surface active dyes at the oil–water interface using fluorescence,^{3,4} resonance Raman scattering,^{5–7} and second harmonic generation (SHG),^{8–10} little is known about the conformation of simple alkyl surfactants at the liquid–liquid interface. Studies of the liquid–liquid interface using surfactant dye molecules alone and in the presence of common ionic surfactants have shown that the dye molecules assume different conformations at varying surface pressures.^{4,11} In addition, fluorescence depolarization studies have shown the importance of surface roughness on the diffusion of molecules on the interface.¹² Recent molecular dynamics calculations have been done that predict molecular ordering at the alkane–water interface.¹³ These calculations coupled with recent SHG studies has led to an understanding of molecular ordering at the interface between a hydrocarbon and an aqueous phase.^{14,15}

In this paper, the ordering of the alkyl chain of sodium dodecyl sulfate (SDS) at the water–carbon tetrachloride interface is examined in detail, by surface sum-frequency generation

(SFG). This technique, pioneered by Shen and co-workers,¹⁶ has been exploited previously, resulting in significant progress in the understanding of many interfacial systems such as solid–adsorbate–air, solid–liquid, and liquid–air interfaces.^{17–31} The inherent advantage of SFG over conventional spectroscopies arises from its dependence on the induced second-order nonlinear polarization, which is generated only in noncentrosymmetric media. This feature makes SFG an ideal technique for studying interfacial systems of centrosymmetric materials, where the symmetry is broken only at the interfacial region. The conformational aspects of adsorption are investigated here by examining the C–H stretching region of the sum-frequency vibrational spectrum with a variety of polarization- and concentration-dependent experiments. A total internal reflection geometry is used which significantly enhances the sensitivity of this technique for the surfactant studied, allowing measurements to be made over a wide range of surface concentrations. Results show that an ordering process takes place for the surfactant at the oil–water interface. In addition, results from deuterated analogues have facilitated assignment of spectral features.

Background

Sum-Frequency Generation. In SFG, two light beams (ω_1 and ω_2) impinge on a surface, generating a light beam of the sum frequency ($\omega_3 = \omega_1 + \omega_2$), the intensity of which is governed by surface polarization.³² Sum-frequency intensities are determined by the induced nonlinear polarization in a media given by

$$P^{(2)}(\omega_{\text{SF}}) = \chi^{(2)} : \hat{e}_{\omega_1} \hat{e}_{\omega_2} \sqrt{I_{\omega_1}} \sqrt{I_{\omega_2}} \quad (1)$$

where $\hat{e}_i = \hat{e}_i f_i$; \hat{e}_i is the unit polarization vector, f_i is the geometric Fresnel factor, I is the laser intensity for each of the input beams ω_1 and ω_2 , and $\chi^{(2)}$ is the second-order polarizability tensor. The resulting sum-frequency intensity is proportional to the square of the induced polarization by

$$I(\omega_{\text{SF}}) = |\tilde{f}_{\text{SF}} P^{(2)}(\omega_{\text{SF}})|^2 \quad (2)$$

where \tilde{f}_{SF} is the nonlinear Fresnel factor for the generated sum-frequency field.

[†] Present address: Department of Chemistry Lehigh University, 6 East Packer Avenue, Bethlehem, PA 18015-3172.

[⊗] Abstract published in *Advance ACS Abstracts*, April 1, 1996.

SFG has been widely used as a spectroscopic probe of interfaces as the hyperpolarizability of adsorbates on the surface strongly affects sum-frequency intensities. The surface polarizability can result from both nonresonant and resonant components. If resonant and nonresonant contributions from the bare interface are negligible, the molecular resonances from the adsorbate will determine the total polarization induced at a surface. In the case of an IR vibrational resonance, the resonant component of the polarizability is given by

$$(\chi_R^{(2)}(\omega_{IR}))_{lmn} = \sum_{\nu} \frac{NA_{n\nu}M_{lm\nu}\Delta p}{\omega_{\nu} - \omega_{IR} - i\Gamma_{\nu}} \quad (3)$$

where N is the adsorbate surface density, $A_{n\nu}$ is the IR transition moment, $M_{lm\nu}$ is the Raman transition strength, Δp is the population difference, ω_{ν} is the transition frequency with a damping constant of Γ_{ν} for a specific transition, ν , and ω_{IR} is the frequency of the incident infrared beam. In the case of sum-frequency vibrational spectroscopy, a tunable IR source is used in combination with a fixed-frequency visible light source. As the IR light is tuned through vibrational resonances, for example the C–H stretch region of the spectrum, the intensity of the emitted sum-frequency signal is dependent on the vibrational modes of the molecules at the interface, resulting in a sum-frequency vibrational spectrum. For a vibrational transition to be sum frequency active it must satisfy the constraint of eq 3 which requires that the vibrational mode be both infrared and Raman active.

Total Internal Reflection. In addition to a strong resonant contribution, the intensity is also dependent upon the Fresnel factors for the input fields, f_i , and the outgoing SF, \tilde{f}_{sf} , as shown in eqs 1 and 2. The detected SF signal is dependent upon the optical properties of the two bulk media through their refractive indices. A comparison of the SF intensity in an internal and external reflection geometry shows that an enhancement of several orders of magnitude is expected for an internal reflection geometry.^{20,22,33–36} For the case of internal reflection, the linear and nonlinear Fresnel factors take on imaginary values at incident angles above the critical angle. The local field intensity exceeds those in an external reflection geometry due to the formation of an evanescent wave at the interface. The maximum in the SF intensity occurs at the critical angles for both incoming fundamental beams. As reported in our initial communication,³¹ this technique is exploited here for the first time to measure the sum-frequency vibrational spectrum of surfactants adsorbed at the liquid–liquid interface. This has allowed the investigation of this interface which has previously been inaccessible by conventional SFG.

Experimental Section

Materials. D₂O (99%) and HPLC grade CCl₄ were purchased from Aldrich. The CCl₄ was further distilled in order to remove any residual hydrocarbon compounds as determined by transmission FTIR. D₂O was shaken with purified CCl₄ prior to use and decanted. Sodium dodecyl sulfate (SDS) (99.8%) was obtained from Aldrich and used as received. Sodium hexadecyl sulfate (SHDS) was prepared by sulfonation of 1-hexadecanol (99%, Aldrich) with chlorosulfonic acid (99%, Aldrich).³⁷ The reaction was carried out by stepwise addition of a solution of chlorosulfonic acid in 1,2-dichloroethane to a solution of 1,2-dichloroethane containing hexadecanol. The reaction was cooled in an ice bath to reduce unwanted side reactions. Sodium bicarbonate was added, and the resulting precipitate was filtered and rinsed with 1,2-dichloroethane. The

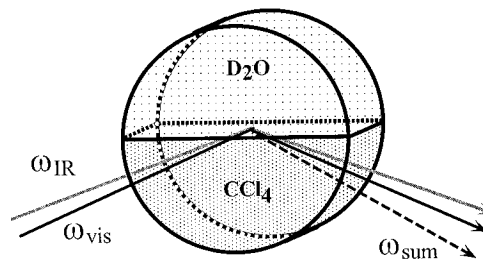


Figure 1. Diagram of the experimental setup and cell design. The infrared (ω_{IR}) and the visible (ω_{vis}) 532 nm beams are incident through the high-index CCl₄ phase.

product was recrystallized from ethanol and characterized by FTIR and proton NMR. Sodium hexadecyl-*d*₃ sulfate was prepared by LiAlH₄ reduction of palmitic-*d*₃ acid in tetrahydrofuran. The resulting alcohol was then sulfonated as above. Purity was determined by FTIR and NMR.

Sum-Frequency Experiments. Tunable IR light was generated using a LiNbO₃ optical parametric oscillator (OPO). The OPO was pumped with the fundamental output of a Q-switched Nd:YAG laser generating 1064 nm pulses at 10 Hz and a pulse duration of 12 ns. Tunability through the desired wavelength region was achieved by angle tuning the crystal. IR radiation in the region 2700–3100 cm⁻¹ with a pulse width of 6 cm⁻¹ at 1–2 mJ was obtained over the entire spectral region. Calibration of the OPO was performed using a polystyrene sample. The remainder of the 1064 nm YAG fundamental was frequency-doubled in a KDP crystal to generate the visible 532 nm.

The sum-frequency experiments were performed using a cylindrical quartz sample cell shown in Figure 1. In order to achieve the desired optical geometry for total internal reflection, both the visible and IR beams were directed onto the interface through the CCl₄, high-index phase, in a copropagating manner. The IR was focused on the interface at an angle of 70°. The visible 532 nm was collimated to a diameter of 1–2 mm and incident on the interface at an angle of 66°. Laser powers used were typically 1–2 mJ/pulse between 2800 and 3100 cm⁻¹ and 5 mJ/pulse at 532 nm.

The sum-frequency signal was collected in reflection at an angle of 66°. The resulting sum-frequency light was polarization selected by a broad-band Glann-Taylor polarizer. The residual 532 nm light was removed by a combination of absorptive, interference, and holographic filters. Detection was accomplished using a PMT and gated electronics. Variation of the input IR polarization was accomplished with a Soleil-Babinet compensator and an IR polarizer. Polarization of the visible light was selected with a half-wave plate. Data points were collected every 2 cm⁻¹ by averaging 200 pulses. The SF spectra were corrected for Fresnel contributions and the intensity variation of the infrared beam throughout the spectral region.

The sample cell used in the SF experiments was cleaned with MicroCleaner and Nochromix solution and rinsed with NANOpure water, which had a resistivity of 17.9 Mohm cm. The cell was dried in an oven at 100 °C to remove residual water. The solvents CCl₄ and D₂O were introduced into the sample cell and allowed to equilibrate. No detectable SF signal was detected from the bare D₂O/CCl₄ interface. This measurement also served as a means of determining the presence of any surface-active contaminants. SDS was added to the cell by removing an aliquot of the D₂O and dissolving the desired amount of SDS. The solution was then returned to the cell and mechanically stirred. SF spectra were collected after allowing the solutions to equilibrate for 20 min. Spectra were collected for concentrations of SDS ranging from 0.1 to 10 mM.

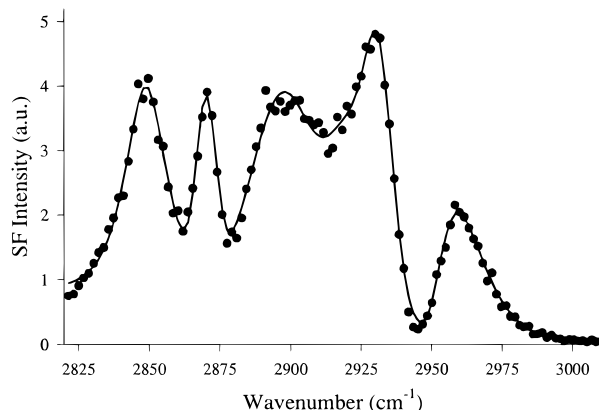


Figure 2. Sum-frequency vibrational spectrum of 5.0 mM SDS at the D_2O-CCl_4 interface. The polarizations used were *p* for visible and *p* for infrared. The sum-frequency output light was collected with no polarization selection. The solid lines represent a fit to the spectra using a combination of Gaussian and Lorentzian functions for each peak.

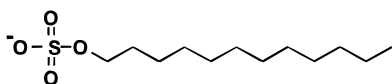


Figure 3. Molecular structure of the surfactant sodium dodecyl sulfate (SDS).

TABLE 1: SFG Peak Frequencies (cm^{-1}) of SDS Adsorbed at the D_2O-CCl_4 Interface and the Measured Infrared and Raman Band Frequencies (cm^{-1}) for Alkyl Chains^{38–43}

SFG		infrared		Raman	
2848	CH_2 SS	2850	$d^+(\pi)$	2850	$d^+(0)$
2872	CH_3 SS	2873	r^+	2871	r^+
2896	CH_2 FR ^a	2890	$d^+(\pi)_{FR}$	2898–2904	$d^+(0)_{FR}$
				2890	$d^-(0)$
2925	CH_2 AS ^a	2928	$d^-(\pi)$	2920–2930	$d^+(0)_{FR}$
2960	CH_3 AS	2953–2962	r^-	2952–2964	r^-

^a See text.

Interfacial Tension Measurements. Interfacial tension measurements were performed using the Wilhelmy plate method. The equipment consisted of an electronic balance equipped with a platinum plate with a resolution of 4 $\mu N/m$. Measurements were performed at the interface of an aqueous solution of SDS and CCl_4 which was allowed to equilibrate for 1 h prior to making a measurement. The neat H_2O/CCl_4 interface was used as a reference in determining the interfacial pressure.

Results and Discussion

Spectral Analysis. Deriving information about molecular conformation and order from the spectral information requires accurate spectral assignments. Such spectral assignments of the SF spectra are aided by comparison with the features of the corresponding infrared and Raman spectra for similar compounds. As was shown in eq 3, a transition must be both IR and Raman active to be SF allowed. Figure 2 displays the SF vibrational spectrum obtained from SDS at the D_2O/CCl_4 interface. The molecular structure of SDS is shown in Figure 3. The spectrum was obtained with a bulk concentration of 5.0 mM with the IR and visible light *p* polarized. No polarization selection was made for the SF output. The peak assignments for SDS are summarized in Table 1. Also shown for comparison are the corresponding infrared and Raman transition frequencies for polymethylene and long-chain alkanes.^{38–43}

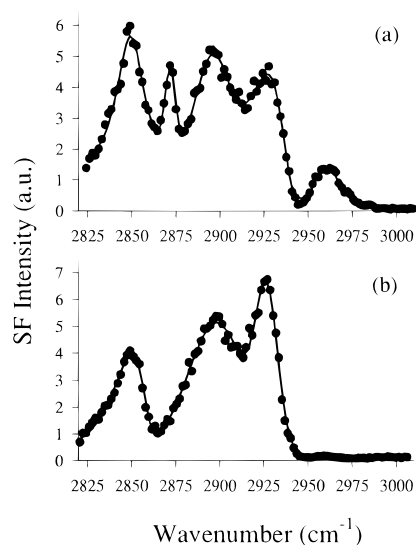


Figure 4. Sum-frequency vibrational spectrum of (a) hexadecyl sulfate, sodium salt, and (b) hexadecyl- d_3 sulfate, sodium salt. The spectra were obtained with *p*-polarized visible, *p*-polarized infrared, and no polarization selection of the output sum-frequency beam. Resonances at 2872 and 2960 cm^{-1} are assigned to the methyl symmetric and asymmetric stretch modes, respectively. The solid lines represent a fit to the spectra using a combination of Gaussian and Lorentzian functions for each peak.

Spectral assignments for the SF spectrum of SDS shown in Figure 2 are made as follows. The peaks at 2872 and 2960 cm^{-1} are assigned to the terminal methyl symmetric and asymmetric stretch modes, respectively. These peaks correspond to the r^+ at 2872 cm^{-1} and r^- at 2963–2953 cm^{-1} , which are seen in both the IR and Raman spectra of polymethylene.^{38–42} The peak at 2848 cm^{-1} is assigned to the CH_2 symmetric stretch (SS) resonance of the hydrocarbon chain. This correlates well with the IR spectrum of an extended polyethylene chain which shows a band at 2850 cm^{-1} for the $d^+(\pi)$ mode.^{38–42} The corresponding Raman spectrum displays a band at 2850 cm^{-1} for the symmetric stretch ($d^+(0)$).^{38–42} The assignment of the peaks in Figure 2 which are centered at 2896 and 2925 cm^{-1} are somewhat more complicated to make. As shown in Table 1, there is a difference between the IR and Raman spectra for these modes. The peak centered at 2896 cm^{-1} is assigned to the symmetric methylene Fermi resonance (FR). This peak appears in the IR ($d^+(\pi)_{FR}$) at 2898–2904 cm^{-1} and in the Raman ($d^+(0)_{FR}$) at 2890 cm^{-1} of polymethylene.^{39,40} It is also possible that there is some degree of a Raman asymmetric methylene mode at 2890 cm^{-1} ($d^-(0)$) that is contributing intensity. The peak at 2925 cm^{-1} is assigned to the methylene asymmetric stretch (AS), in agreement with the value observed in the IR spectrum (2928 cm^{-1}),³⁸ although previous Raman studies have assigned a peak at 2890 cm^{-1} to the methylene asymmetric stretch.³⁹ It is possible that intensity from the methylene Fermi resonance ($d^+(0)_{FR}$) may contribute to this peak. Previous SFG studies have assigned a peak at 2930–2940 cm^{-1} to a Fermi resonance resulting from interaction of an overtone of the CH_3 bending mode with the methyl symmetric stretch.^{23,24,44–47} However, this peak is not observed in the present SF spectrum of SDS.

These assignments have been further verified by deuteration studies. Figure 4a,b displays the SF spectra obtained from sodium hexadecyl sulfate (SHDS) and hexadecyl- d_3 sulfate, sodium salt, for which the terminal methyl group has been deuterated. The most striking change between parts a and b of Figure 4 is the disappearance of the methyl peaks at 2872 and 2960 cm^{-1} for the symmetric and asymmetric modes, respec-

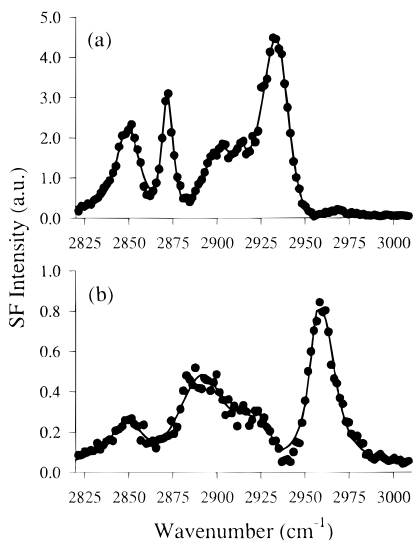


Figure 5. Sum-frequency vibrational spectra of sodium dodecyl sulfate with (a) s-polarized output, s-polarized visible, and p-polarized infrared and (b) s-polarized output, p-polarized visible, and s-polarized infrared. Spectra were obtained with a solution of 5.0 mM SDS in D_2O . The solid lines represent a fit to the spectra using a combination of Gaussian and Lorentzian functions for each peak.

tively. Comparison of the spectra in Figure 4a,b also shows that no detectable peak arising from the methyl Fermi resonance is observed. There has been some discrepancy in the past as to the exact assignment of the CH_2 asymmetric stretch and the Fermi resonance of the methyl stretch which both occur in the region of $2920\text{--}2940\text{ cm}^{-1}$.^{31,46} The assignments obtained from these deuteration studies establish that this peak is dominated by the methylene asymmetric mode with the possibility that intensity from the CH_3 Fermi resonance may also contribute slightly. This assignment is in contrast to SFG spectra from self-assembled on metal substrates⁴⁴ and Langmuir–Blodgett films of cadmium arachidate on fused silica,^{23,48} where this Fermi resonance is pronounced. The assignments for SDS at the $D_2O\text{--}CCl_4$ interface are consistent with SF spectra obtained from other liquid surfaces such as alcohols and alkanes at the water–air interface.⁴⁹

The local symmetry of the CH_2 hydrocarbon backbone plays an important role in the determination of peak intensities of the CH_2 resonances. Under the dipole approximation for SFG, little contribution from methylene resonances should be observed for a system of well-ordered (all-trans) hydrocarbon chains.¹⁸ It is well-known that although there is an odd number of methylene groups, essentially no signal arises from the methylenes in a well-ordered system.^{18,47} The presence of a large methylene intensity therefore suggests a significant number of gauche defects in the hydrocarbon chain which relax the local symmetry constraint. The terminal methyl, which possesses both IR- and Raman-active modes, is by nature in a noncentrosymmetric environment regardless of chain conformation. Conformational information can be obtained from the relative intensity of the methyl peaks which reflect the orientational average of the ensemble with respect to the surface normal. For example, polarization dependence of the symmetric methyl stretch has been used in the past as a means of determining the average tilt angle of the hydrocarbon chain in these systems.¹⁸

Polarization Studies. The spectra of SDS shown in Figure 5a,b are obtained with the polarization combinations of ssp (s-polarized SF, s-polarized visible, p-polarized IR) and sps (s-polarized SF, p-polarized visible, s-polarized IR), respectively. The spectra in Figure 5a,b have been corrected for Fresnel contributions over the spectral region displayed. With ssp

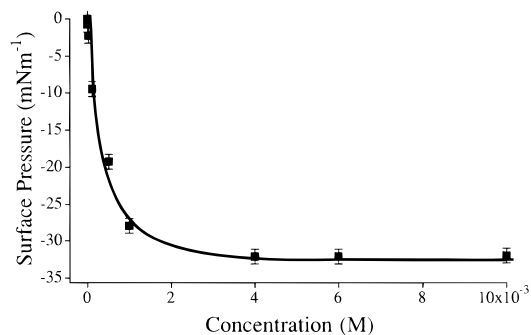


Figure 6. A plot of the interfacial pressure of sodium dodecyl sulfate at the water–carbon tetrachloride interface versus the aqueous concentration of sodium dodecyl sulfate. Measurements were obtained using the Wilhelmy plate method. Interfacial pressures were calculated by subtracting the value of the interfacial tension of the neat $D_2O\text{--}CCl_4$ interface. The solid line is shown as a guide to the eye.

polarization only the normal component of the vibrational transition moments will contribute to the observed intensity, and similarly for sps polarization, only the components parallel to the surface will be active. For the terminal methyl group, which possesses C_{3v} symmetry, the transition dipoles of the symmetric and asymmetric stretches are orthogonal to each other. For the case of ssp polarization, in which the C_{3v} axis of the terminal methyl is assumed to lie along the surface normal, only the symmetric stretch peak will be apparent with no appreciable intensity due to the asymmetric stretch. However, if the symmetry axis of the terminal methyl lies parallel to the surface, the CH_3 symmetric stretch will have no intensity, and the asymmetric stretch will dominate.

The spectra in Figure 5a of SDS at a concentration of 5.0 mM for ssp polarization (p-polarized IR) shows a pronounced CH_3 symmetric stretch at 2872 cm^{-1} with negligible intensity of the CH_3 asymmetric resonance at 2960 cm^{-1} . This suggests that the terminal methyl group is pointing primarily along the surface normal which is also substantiated by Figure 5b. For the sps polarization (s-polarized IR) displayed in Figure 5b, the symmetric stretch of the terminal methyl is completely absent, and the most prominent feature in this spectra is the asymmetric CH_3 mode. These results, which are found for the entire concentration range of SDS examined (0.1–10 mM), unambiguously support the conclusion that the terminal methyl group is oriented normal to the surface. Any conclusions regarding the absolute orientation or orientational average of the alkyl chain, however, are complicated by the fact that there appears to be a large number of gauche defects in the alkyl chains as seen by the strong symmetric methylene peak of Figures 2 and 5a.

Concentration Studies. To investigate surface coverage effects on surfactant conformation, SF spectra were collected for a series of aqueous surfactant concentrations. Spectra were taken from 0.1 to 10.0 mM bulk SDS concentration in D_2O . Surface coverages were estimated using interfacial pressure measurements with the results shown in Figure 6. The minimum tension achieved at 2.0 mM bulk concentration is taken to reflect a surface coverage of one monolayer. Above this concentration, the surface pressure does not change.

As was discussed previously, the methyl and methylene region of the infrared spectrum is especially indicative of the conformational ordering of the surfactant alkyl chain. The methyl and methylene region of the vibrational spectra of SDS for 0.1 and 10.0 mM using ssp polarization is shown in Figure 7. In this figure, strong C–H resonances are observed for both the methyl and methylene symmetric stretch. Even at a relatively low surface coverage, a high signal-to-noise ratio is

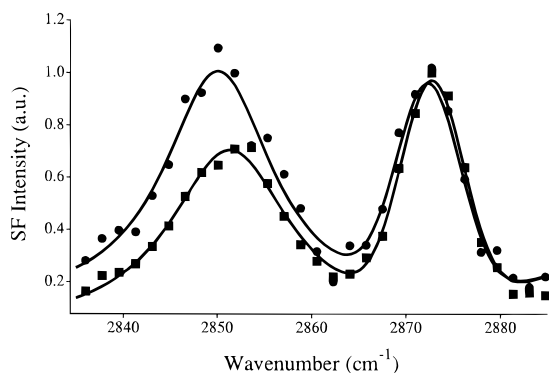


Figure 7. Sum-frequency vibrational spectrum of the symmetric stretch region for sodium dodecyl sulfate at the D_2O-CCl_4 interface. Spectra are shown for 0.1 (●) and 10 mM (■) SDS aqueous concentration. The spectra were taken using s-polarized output, s-polarized visible, and p-polarized infrared. The solid lines represent a fit to the spectra using a combination of Gaussian and Lorentzian functions for each peak.

observed, establishing the very high sensitivity of this technique. Two features in this data warrant further discussion. First, the presence of a strong methylene peak necessarily leads to the conclusion that a number of gauche defects exist in the chain throughout the concentration region examined, corresponding to a small fraction of a monolayer to one full monolayer. This result shows that the surfactant molecules at the D_2O-CCl_4 interface do not attain a well-ordered all-trans configuration at even full monolayer coverage. This result is in contrast to many other monolayer systems in which full monolayer coverage corresponds to an all-trans close-packed configuration for the alkyl chains.^{18,24,50} However, at the liquid-liquid interface, solvent interaction between the carbon tetrachloride and the alkyl portion of the surfactant molecules likely weakens the chain-chain interactions which are responsible for the all-trans ordering of the alkyl backbone during packing induced ordering. Other processes responsible for ordering at an interface such as physisorption or chemisorption of the adsorbate onto a solid substrate are not possible at a liquid-liquid interface. In addition, mechanical compression of an insoluble monolayer is not possible because the adsorbate is in dynamic equilibrium with the bulk solution.

The second interesting aspect of the data in Figure 7 is the change in relative intensity of the symmetric methyl and methylene peaks with bulk concentration. A decrease in the methyl to methylene intensity ratio is observed with increased concentration, suggesting a change in the conformation of the alkyl chain. A variation in this ratio indicates a change in orientation of the average component of the methyl and methylene transition dipole along the surface normal. The polarization data presented previously have shown that the C_{3v} axis of the methyl group lies primarily along the z axis, and this holds true for all concentrations examined. This observation suggests that no net change in methyl orientation occurs, but rather a change in methylene chain conformation is causing the observed variation in the CH_3/CH_2 ratio. With the infrared light beam polarized along the z axis, an increase in the ratio most likely reflects a decrease in the CH_2 symmetric stretch intensity, indicating that the alkyl chains are assuming a conformation that contains fewer gauche defects, not simply a change in tilt angle or orientation along the surface normal. This allows one to use the methyl/methylene symmetric stretch intensity ratio as an indicator of the relative order within the chains for various concentrations. A low methyl to methylene ratio reflects a relatively small amount of order in the alkyl chain consisting of a relatively large amount of gauche defects in the alkyl chain.

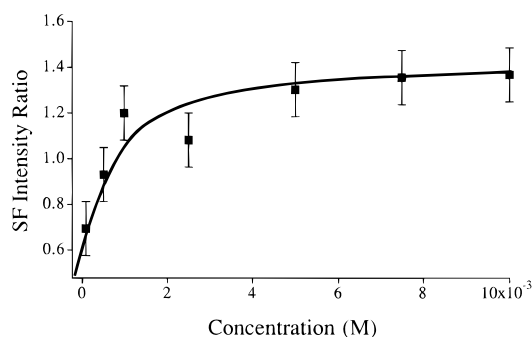


Figure 8. A plot of the ratio of methyl symmetric stretch peak intensity to the methylene symmetric stretch peak intensity versus bulk aqueous concentration.

The ratio of the methyl to methylene peak intensity, for the range of concentrations examined, is plotted in Figure 8. At low concentrations, a relatively low ratio is observed which increases significantly with increased adsorption at the interface. This ratio reaches a maximum at one monolayer coverage, corresponding to 2.0 mM aqueous concentration. These results suggest that the chains become more ordered (fewer gauche defects) as more surfactant adsorbs to the interface. An ordering of the alkyl chains may be caused by a closer packing of molecules on the surface. The favorable energetics of the anionic head groups occupying interfacial sites will further force the hydrophobic alkyl chains to be driven away from the interface as surface sites become limited. This process will necessitate a more ordered configuration with more trans bonds within the alkyl chain. Such ordering processes have been observed at the air-liquid and solid-air interface.^{18,50} At the air-liquid interface, molecules forming insoluble monolayers can be physically restricted to a small surface area by mechanical compression.⁵¹ Previous spectroscopic investigations by SFG of Langmuir monolayers of pentadecanoic acid on water in fact show a close correlation between molecular area and alkyl chain disorder.¹⁸ Other studies by FTIR on solid substrates⁵⁰ have shown similar results for assembled molecules on solid supports.

Another important result of these concentration studies pertains to information on the extent of the spatial region that is probed by this technique. The evanescent wave generated at the interface by the incoming light field decays into the low-index medium exponentially with distance, generating a large electric field in the low-index material up to microns from the interfacial region. It is often unclear what the actual depth of the sum-frequency active region at an interface between two centrosymmetric materials is. Recent SFG experiments⁴⁹ have confirmed that the majority of SF signal arises from interfacial region and that no measurable amount of signal arises from the bulk material. This work confirms these conclusions for this system. Changes in the SF spectral features with concentration closely follow changes in interfacial pressures, suggesting that SF is probing only the interfacial region. This is consistent with the highly surface specific description of SFG.

Disorder in alkyl chains induced by laser heating has been observed in a study of Langmuir-Blodgett films on CaF_2 using SFG.⁵² To rule out the possibility that this heating may contribute to observed ordering effects, spectra were taken with and without probing the methylene stretch excitation which is thought to contribute to chain disorder. Identical spectra were observed, showing that laser heating is not causing disorder in this particular system. A plausible explanation for this is that the fluid nature of the monolayer at the liquid-liquid interface allows the monolayer to restructure and dissipate heat more effectively than that of a solid-air interface.

Conclusions

With the use of TIR SFG the first vibrational spectrum of the simple alkyl surfactant sodium dodecyl sulfate at the D₂O–CCl₄ interface has been obtained. By performing these experiments in a TIR geometry, the sensitivity of the surface selective technique of SFG is increased considerably. Infrared and Raman spectra for similar compounds were used to assign the C–H vibrational resonances of the SF spectra of SDS. Spectral assignments were further verified by deuteration studies. The SF spectra of sodium hexadecyl sulfate was compared with sodium hexadecyl-*d*₃ sulfate in order to determine the contribution from the terminal methyl group to the SF spectra of SDS. Deuteration results reveal that, unlike monolayers adsorbed to solid substrates, minimal contribution from the methyl Fermi resonance is observed.

TIR SFG has allowed for the investigation of conformational and orientational ordering of SDS at the D₂O–CCl₄ interface. The ratio of the methyl/methylene intensity as a function of bulk concentration is used as a measure of chain conformation. By normalizing consecutive spectra to the symmetric methyl peak to correct for concentration effects, a decrease in the methylene intensity is observed, suggesting a reduction in gauche defects. This finding is consistent with increased ordering with increased surface coverage. The surface pressure and the methyl/methylene intensity ratio both reach a constant value at 2.0 mM, which is taken as the formation of a full monolayer.

Polarization studies were also performed in order to ascertain the orientation of SDS at the D₂O–CCl₄ interface. These SFG studies suggest that the C_{3v} symmetry axis of the terminal methyl group is oriented primarily along the surface normal for all concentrations examined. The CH₂ backbone displays pronounced resonances due to the symmetric and asymmetric methylene modes at 2848 and 2925 cm⁻¹, respectively. The large intensity observed for these resonances is the result of the relaxation of the local symmetry constraint for the CH₂ vibrations by the introduction of gauche defects.

Historically, an investigation of molecular species adsorbed at a liquid/liquid phase boundary by conventional vibrational spectroscopy has been inaccessible. Complications arising from distinguishing between the spectral contributions of interfacial molecules and those in the more pervasive bulk have presented a formidable experimental challenge. These limitations have been overcome by the use of the surface selective technique of TIR SFG. The results reported here have far-reaching implications for the investigation of adsorption and transport properties at the interface between two immiscible liquids by vibrational spectroscopy.

Acknowledgment. The authors gratefully acknowledge the skilled assistance of Jennifer Gage and the facilities provided by Professor Bruce Branchaud for the synthesis of hexadecyl-*d*₃ sulfate, sodium salt. In addition, the authors express appreciation to Ted Hinke for the construction of the cell. The starting material palmitic-*d*₃ acid was graciously provided by Professor Frederick Dahlquist. Funding is gratefully acknowledged from NSF (CHE 9416856) and the Office of Naval Research.

References and Notes

- (1) Hiemenz, P. C. *Principles of Colloid and Surface Chemistry*; Marcel Dekker: New York, 1977; Vol. 4.
- (2) Myers, D. *Surface, Interfaces and Colloids; Principles and Applications*; VCH: New York, 1991.
- (3) Wirth, M. J.; Burbage, J. D. *J. Phys. Chem.* **1992**, *96*, 9022.
- (4) Piasecki, D. A.; Wirth, M. J. *J. Phys. Chem.* **1993**, *97*, 7700.

- (5) Takenaka, T. T.; Nakanaga, T. *J. Phys. Chem.* **1976**, *80*, 475.
- (6) Tian, Y.; Umemura, J.; Takenaka, T. *Langmuir* **1988**, *4*, 1064.
- (7) Takenaka, T. *Chem. Phys. Lett.* **1978**, *55*, 515.
- (8) Grubb, S. G.; Kim, M. W.; Rasing, T.; Shen, Y. R. *Langmuir* **1988**, *4*, 452.
- (9) Higgins, D. A.; Corn, R. M. *J. Phys. Chem.* **1993**, *97*, 489.
- (10) Higgins, D. A.; Naujok, R. R.; Corn, R. M. *Chem. Phys. Lett.* **1993**, *213*, 485.
- (11) Nakanaga, T.; Takenaka, T. *J. Phys. Chem.* **1977**, *81*, 645.
- (12) Kovaleski, J. M.; Wirth, M. J. *J. Phys. Chem.* **1995**, *12*, 4091.
- (13) van Buuren, A. R.; Marrink, S.-J.; Berendsen, H. J. C. *J. Phys. Chem.* **1993**, *97*, 9206.
- (14) Conboy, J. C.; Daschbach, J. L.; Richmond, G. L. *Appl. Phys. A* **1994**, *42*, 237.
- (15) Conboy, J. C.; Richmond, G. L. *J. Phys. Chem.* **1994**, *98*, 9688.
- (16) Shen, Y. R. *Nature* **1989**, *337*, 519.
- (17) Hunt, J. H.; Guyot-Sionnest, P.; Shen, Y. R. *Chem. Phys. Lett.* **1987**, *133*, 189.
- (18) Guyot-Sionnest, P.; Hunt, J. H.; Shen, Y. R. *Phys. Rev. Lett.* **1987**, *59*, 1597.
- (19) Bain, C. D. *J. Chem. Soc., Faraday Trans.* **1995**, *91*, 1281.
- (20) Miragliotta, J.; Polizzotti, R. S.; Rabinowitz, P.; Cameron, S. D.; Hall, R. B. *Chem. Phys.* **1990**, *143*, 123.
- (21) Hall, R. B.; Russell, J. N.; Miragliotta, J.; Rabinowitz, P. R. *Springer Ser. Surf. Sci.* **1990**, *22* (*Chem. Phys. Solid Surf.* *8*), 87.
- (22) Hatch, S. R.; Polizzotti, R. S.; Dougal, S.; Rabinowitz, P. *J. Vac. Sci. Technol.* **1993**, *11*, 2232.
- (23) Akamatsu, N.; Domen, K.; Hirose, C.; Onishi, T.; Shimizu, H.; Masutani, K. *Chem. Phys. Lett.* **1991**, *181*, 175.
- (24) Hirose, C. Y.; Yamamoto, H.; Akamatsu, N.; Domen, K. *J. Phys. Chem.* **1993**, *97*, 10064.
- (25) Wolfrum, K.; Graener, H.; Laubereau, A. *Chem. Phys. Lett.* **1993**, *213*, 41.
- (26) Wolfrum, K.; K.; Lobau, J.; Laubereau, A. *Appl. Phys. A* **1994**, *59*, 605.
- (27) Zhang, D.; Gutow, J.; Eienthal, K. B. *J. Phys. Chem.* **1994**, *98*, 13729.
- (28) Harris, A. L.; Levinos, N. J.; Rothberg, L.; Dobois, L. H.; Dhar, L.; Shane, S. F.; Morin, M. *J. Electron Spectrosc. Relat. Phenom.* **1990**, *54–55*, 5.
- (29) Harris, A. L.; Rothberg, L. *J. Chem. Phys.* **1991**, *94*, 2449.
- (30) Harris, A. L.; Rothberg, L.; Dhar, L.; Levinos, N. J.; Dubois, L. H. *J. Chem. Phys.* **1991**, *94*, 2438.
- (31) Messmer, M. C.; Conboy, J. C.; Richmond, G. L. *J. Am. Chem. Soc.* **1995**, *117*, 8039.
- (32) Shen, Y. R. *The Principles of Nonlinear Optics*; Wiley: New York, 1984.
- (33) Dick, B.; Gierulski, A.; Marowsky, G. *Appl. Phys. B* **1987**, *42*, 237.
- (34) Bloembergen, N.; Pershan, P. S. *Phys. Rev.* **1962**, *128*, 606.
- (35) Bloembergen, N. *Opt. Acta* **1966**, *13*, 311.
- (36) Bloembergen, N.; Simmon, H. J. *Phys. Rev.* **1969**, *181*, 1261.
- (37) Fieser and Fieser; *Reagents for Organic Synthesis*; Wiley: New York, 1967.
- (38) Snyder, R. G.; Hsu, S. L.; Krimm, S. *Spectrochim. Acta* **1978**, *34A*, 395.
- (39) Snyder, R. G.; Strauss, H. L.; Elliger, C. A. *J. Phys. Chem.* **1982**, *86*, 5145.
- (40) MacPhail, R. A.; Strauss, H. L.; Snyder, R. G.; Elliger, C. A. *J. Phys. Chem.* **1984**, *88*, 334.
- (41) Cates, D. A.; Strauss, H. L.; Snyder, R. G. *J. Phys. Chem.* **1994**, *98*, 4482.
- (42) Snyder, R. G.; Scherer, J. R. *J. Chem. Phys.* **1979**, *71*, 3221.
- (43) Aljibury, A. L.; Snyder, R. G.; Strauss, H. L.; Raghavachari, K. *J. Chem. Phys.* **1986**, *84*, 6873.
- (44) Bain, C. D.; Davies, P. B.; Ong, T. H.; Ward, R. N.; Brown, M. A. *Langmuir* **1991**, *7*, 1563.
- (45) Bain, C. D. *Langmuir* **1994**, *10*, 2060.
- (46) Ward, R. N.; Duffy, D. C.; Davies, P. B.; Bain, C. D. *J. Phys. Chem.* **1994**, *98*, 8536.
- (47) Guyot-Sionnest, P.; Superfine, R.; Hunt, J. H.; Shen, Y. R. *Chem. Phys. Lett.* **1988**, *144*, 1.
- (48) Akamatsu, N.; Domen, K.; Hirose, C. *J. Phys. Chem.* **1993**, *97*, 10070.
- (49) Sefler, G. A.; Du, Q.; Miranda, P. B.; Shen, Y. R. *Chem. Phys. Lett.* **1995**, *235*, 347.
- (50) Golden, W. G.; Snyder, C. D.; Smith, B. *J. Phys. Chem.* **1982**, *86*, 4675.
- (51) Roberts, G. *Langmuir-Blodgett Films*; Plenum Press: New York, 1990.
- (52) Goto, Y.; Akamatsu, N.; Domen, K.; Hirose, C. *J. Phys. Chem.* **1995**, *99*, 4086.